https://ntrs.nasa.gov/search.jsp?R=19690024068 2018-07-25T13:24:16+00:00Z

NASA CR 103846

NATIONAL AERONAUTICS AND SPACE ADMINISTRATION

Technical Report 32-1388

Tensile Creep-Rate Studies on Pyrolytic Carbon

D. B. Fischbach

CASE FILE COPY

JET PROPULSION LABORATORY
CALIFORNIA INSTITUTE OF TECHNOLOGY
PASADENA, CALIFORNIA
July 15, 1969

NATIONAL AERONAUTICS AND SPACE ADMINISTRATION

Technical Report 32-1388

Tensile Creep-Rate Studies on Pyrolytic Carbon

D. B. Fischbach

JET PROPULSION LABORATORY
CALIFORNIA INSTITUTE OF TECHNOLOGY
PASADENA, CALIFORNIA
July 15, 1969

Prepared Under Contract No. NAS 7-100
National Aeronautics and Space Administration

Preface

The work described in this report was performed by the Engineering Mechanics Division of the Jet Propulsion Laboratory.

Contents

I. Introduction 1

II. Experimental Materials and Techniques 3

III. Results 5

IV. Discussion 12

V. Summary and Conclusions 16

References 17

Table

1. Creep recovery behavior of pyrolytic carbon 11

Figures

1. Microstructure of pyrolytic carbon normal to substrate. 4
2. Distribution of stress and elongation in specimen as function of distance from center in units of total length. 6
3. Reduction in gage cross-section area as a function of gage elongation. 6
4. Dependence of recorded creep rate on recorded creep strain at representative temperatures and stresses 7
5. Portion of a typical creep curve showing stress changes and creep-rate values (2600°C) 8
6. Recorded creep rate as a function of recorded creep elongation at several stress levels on a single specimen at 2700°C 9
7. Recorded creep rate as a function of stress at $\epsilon_c \sim 25\%$ 9
8. Stress exponent n as a function of recorded creep elongation for various specimens in various temperature ranges 10
9. Recorded creep rate as a function of recorded creep elongation at various temperatures at a stress of $\sim$15,000 psi on a single specimen 10
10. Creep hardening rate h as a function of temperature 11

Abstract

The parallel-to-substrate tensile creep behavior of an as-deposited (2200°C), substrate-nucleated, pyrolytic carbon was investigated over the temperature range 2500–2900°C and the stress range 5000–30,000 psi under deadweight loading. A stress-change technique was combined with a graphical-interpolation analysis to obtain data on the stress σ and temperature T dependence of the creep rate $\dot{\epsilon}$ over broad strain ϵ and stress or temperature ranges on individual specimens. These data were used to determine the stress exponent n and the activation energy ΔH in the empirical expression $\dot{\epsilon} = A\sigma^n \exp(-\Delta H/RT)$. Two distinct deformation regimes were confirmed. After 1–2% gage elongation, an increase in $\dot{\epsilon}$ indicated a change in deformation mechanism. In the same range, n dropped from an initial value of $\sim$4 to 1.5 $\pm$0.4, where it remained to at least 30% elongation independent of T and σ. In agreement with other results on deformation and graphitization of graphitizing carbons and graphite, $\Delta H =$ 250 $\pm$40 kcal/mole. During the first 8% elongation, several changes occurred in structure and properties. A density increase of $\sim$2% and a large increase in Young's modulus were produced by the graphitization and preferred orientation increase (reported elsewhere) that occur in this range. The reduction in area showed that, aside from the graphitization volume decrease, the deformation occurred at constant volume to at least 30% elongation. After the early anomaly, $\dot{\epsilon}$ decreased regularly with increasing ϵ. Creep recovery was small, and appeared to decrease with increasing preferred orientation. The first stage of deformation was dominated by breakdown of the as-deposited structure, evidently involving dislocation glide and climb. Among various mechanisms considered for the second-stage deformation, which occurs in highly oriented, well-graphitized material, self-diffusion mass transport was most consistent with the observations.

Tensile Creep-Rate Studies on Pyrolytic Carbon

I. Introduction

Although carbons and graphites are brittle at low and moderate temperatures, significant ductility and increased strength occur at elevated temperatures. This means that mechanisms of plastic deformation that are inoperative at low temperatures become effective at high temperatures. In this respect—despite important differences in detailed aspects, such as fracture elongation, tensile strength, and reduction in area—there are strong qualitative similarities in the behavior of the whole range of nominally pure, natural and synthetic carbon and graphite materials. Considerable data exist on the high-temperature mechanical behavior, but there is as yet little understanding of the basic mechanisms of plastic deformation and failure in these materials.

Ideally, investigations of fundamental mechanisms should begin with ideal materials; i.e., near-perfect single crystals. Unfortunately, good-quality single crystals of graphite are not readily available, and their size is invariably small. This makes high-temperature mechanical studies very difficult. On the other hand, the microstructural heterogeneity of common binder–filler synthetic graphites makes them undesirable materials for fundamental studies. At JPL, therefore, attention has been concentrated upon pyrolytic carbon (PC), also called pyrolytic graphite, as a model material representative of the broad class of graphitizing carbons and graphites.

Pyrolytic carbon is formed by the thermal decomposition of hydrocarbon vapor (usually methane) and deposition of the resultant carbon on a hot substrate at temperatures in the range 1900–2300°C. Such PCs are very pure, with near-theoretical density and a strong, preferred-orientation texture (with layer planes approximately parallel to the substrate). Although the as-deposited structure is turbostratic (disordered layer stacking), PCs graphitize quite completely under the influence of high-temperature thermal and mechanical treatment. Therefore, they are well-suited to fundamental studies of processes that occur in graphitizing carbons and in graphite; they are also materials of considerable importance to the aerospace industry.

In a recent paper (Ref. 1), a large body of information on the parallel-to-substrate tensile stress–strain, tensile creep, and basal-shear behavior of PCs was analyzed for the purpose of identifying fundamental deformation mechanisms in graphite. This analysis disclosed that the deformation of as-deposited PC is characterized by two distinct regimes.

Initially, in stage I (with tensile strains parallel to the substrate less than about 10%), a microstructural transformation—analogous in some ways to recrystallization phenomena in metals—dominates the plastic behavior. The as-deposited, turbostratic, wrinkled-sheet structure is broken down and transformed into a well-graphitized, very highly oriented structure (Refs. 2 and 3).

Subsequent tensile elongation in stage II (with strains in excess of 10%) occurs, therefore, in a highly anisotropic, polycrystalline graphite that resembles single-crystal material in many of its properties. In both stage I and stage II, tensile reduction in the cross-sectional area was found to be approximately the constant-volume value, and there was no indication of necking. Changes in cross-sectional dimensions of the uniform-gage section, as a function of elongation parallel to the substrate, were particularly revealing (Refs. 1 and 4), and have been reexamined in a subsequent report (Ref. 5). During first-stage deformation, the width (parallel to substrate, perpendicular to stress) increased and the thickness (perpendicular to both substrate and stress) decreased in a manner appropriate to the *dewrinkling* of the structure that accompanied the deformation. During the second stage, the width and thickness decreased at the same rate, *in the manner expected for an isotropic material.*

For the mechanisms of high-temperature plasticity in graphite, these results have very important implications. Simple shear, kinking, and twinning of the basal planes—long recognized as important modes of deformation in single-crystal graphite—cannot account for the observed tensile behavior of well-graphitized, highly oriented PC. Mechanisms are required that provide compressive plasticity normal to the basal planes (parallel to the c-axis) and tensile plasticity within the basal planes.

A number of such mechanisms can be suggested (Refs. 1, 2, and 4). One obvious and attractive possibility is the glide of nonbasal dislocations, especially on pyramidal-type slip planes. Abundant evidence is now available for the existence of a variety of types of nonbasal dislocations in graphite (Refs. 6 and 7). However, little information exists regarding the mobility and other properties of such dislocations; no slip bands, or other convincing micrographic evidence of nonbasal dislocation glide, have been reported; and the reported dislocation densities are very low for an important deformation mechanism. Alternatively, it could be supposed that interleaved packets of incomplete or fractured basal planes pull apart in a basal shear mode, and that the resultant interlaminar cracks heal by collapse of adjacent layers, to maintain a high density. Such a mechanism appears to be generally consistent with available information on the microstructure and strength of PCs, and could account (at least qualitatively) for the observed decrease in gage-section thickness. However, it is difficult to account for the width decrease by this mechanism.

A more general deformation mechanism, which deserves serious consideration, is diffusion mass-transport of the Nabarro–Herring type, either between crystallite boundaries or between more localized defects within the crystallites. Such a mechanism is consistent with the small apparent crystallite size (a few hundred to a few thousand angstroms) and the apparent thermally activated character of the deformation. Furthermore, it could provide plasticity both parallel and perpendicular to the c-axis. Lack of information on a number of important features, such as stress-dependence of the creep rate, has precluded any firm conclusions as to the relevance of this mechanism to graphite.

In summary, although the known deformation characteristics of graphite impose on the mechanisms important restrictions, present information is insufficient to isolate the actual operating modes from a variety of possible modes.

In principle, the stress-dependence of the creep rate offers a simple technique for distinguishing between various possible deformation mechanisms. The following empirical expression is characteristic of the operating deformation mechanism:

$$\dot{\epsilon} = A\sigma^n \tag{1}$$

where

$\dot{\epsilon}$ = creep rate

σ = stress

A = a temperature-dependent (and perhaps strain-dependent) function of the material

n = stress exponent

For a dislocation climb mechanism, such as is found in many metals, $n \geqslant 4$ is expected, whereas a viscous mechanism, such as Nabarro–Herring creep, should give $n = 1$. This technique has been applied to a number of binder–filler synthetic graphites, including conventional coke–pitch graphite (Ref. 8), a uranium-loaded graphite (Ref. 9), and a well-oriented, stress-recrystallized graphite (ZTA), as cited in Refs. 10 and 11. For all of these materials, very high values of n in the range 5.5–8 were found in both tension and compression.

The fundamental significance of these results is difficult to interpret. Well-known characteristics of such binder–filler graphites are the small reduction in area and the significant decrease in bulk density that accompany tensile deformation. This means that the observed macroscopic tensile strain results more from an increase in void volume than from any true, homogeneous plasticity. The actual plastic deformation is highly localized and heterogeneous on a scale commensurate with the grain size of the material. This has been demonstrated explicitly in an elegant series of experiments by Green and associates (Ref. 11 and 12). Consequently, the observed strain rate and nominal stress bear an unknown and possibly a complex relationship to the stress and strain-rate relationship in the actual plastic zones. In compression, the experimental situation is better, but it is reasonable to expect that here, too, the rate-limiting deformation occurs very heterogeneously in these materials.

Reasonably homogeneous plasticity is, therefore, a highly desirable prerequisite for fundamental deformation-mechanism studies based upon gross behavior such as creep rate. A simple test for this is constant-volume reduction in area. One carbon material that adequately fulfills this criterion is glassy (vitreous) carbon, which is a hard, isotropic, nongraphitizing carbon. The stress- and temperature-dependence of the creep rate in glassy carbon has recently been discussed elsewhere (Refs. 13 and 14).

Another such material is PC. Earlier work at JPL on creep of PC was primarily concerned with temperature-dependence and microstructural aspects of the deformation of annealed material (Ref. 15). The present report deals with the stress-dependence and other aspects of the tensile creep rate of as-deposited and (tensile) hot-worked PC. The objective of this research was an extension of the understanding of the high-temperature plastic behavior of PC and of graphites in general, with particular attention given to identification of the fundamental mechanisms of deformation. Preliminary reports on some of the results have been published elsewhere (Refs. 5, 14, and 16).

II. Experimental Materials and Techniques

All of the data were taken on samples machined from a single lot of PC obtained from a commercial supplier.* The carbon was deposited from methane at 2200°C, and had a basically substrate-nucleated structure, as shown in Fig. 1a. The original plates, which were about 0.5 in. thick, were cleaved into three pieces of the same thickness. Machined from this material were dogbone-type tensile specimens, with a 0.100 × 0.080 × 0.75-in.^{3} uniform-gage section, that blended smoothly into a 0.75-in.-radius throat and grip section. These specimens were tested in the as-deposited condition. The characteristic microstructural changes induced by heat treatment and tensile deformation are shown in Fig. 1b, c, and d.

Basically, the test equipment was the same as that used in earlier JPL carbon- and graphite-deformation studies (Refs. 17 and 18), with several minor but significant modifications (see Ref. 13). The split, coke–pitch graphite grips were fitted with glassy carbon inserts in the region where they contacted and transferred the load to the specimen. These hard, relatively high-modulus inserts bridged the separation between the grip halves, preventing specimen extrusion through the gap, distributing the stress over a larger area of the grip, and providing a dimensionally stable load-transfer interface between grip and specimen. In this way, grip-deformation effects were substantially reduced. The grips were coupled to the carbon load-train rods through spherical-seat joints. A special jig was used to assemble the load train and to mount the specimen in the grips; a removable rigid clamp, bridging the two grips, prevented accidental damage to the specimen during load-train installation in and removal from the creep apparatus. Multiple tests on a single specimen, with removal and examination after each test, could be carried out routinely without difficulty or risk of specimen breakage.

The assembled load train was suspended in the furnace from a load cell, and the lower end was passed through a guide bearing and clamp assembly before attaching to the load pan. Using a ball-screw jack, the load was applied and removed smoothly and rapidly; the pan was so designed that the load could be applied in two increments of variable size. The size of the secondary load could be adjusted while the specimen crept under the primary load, thus facilitating the investigation of stress-dependence effects over a broad stress range by a stress-change technique. All tests were made under deadweight rather than constant-stress conditions. The tare load was equivalent to a stress on the specimen of about 500 psi.

Temperatures as high as 2900–3000°C in helium, at approximately 1 atm, were provided by an automatically controlled, graphite tube resistance furnace. For control purposes, the temperature was sensed by a radiation

*Super Temp Corp., Santa Fe Springs, Calif.

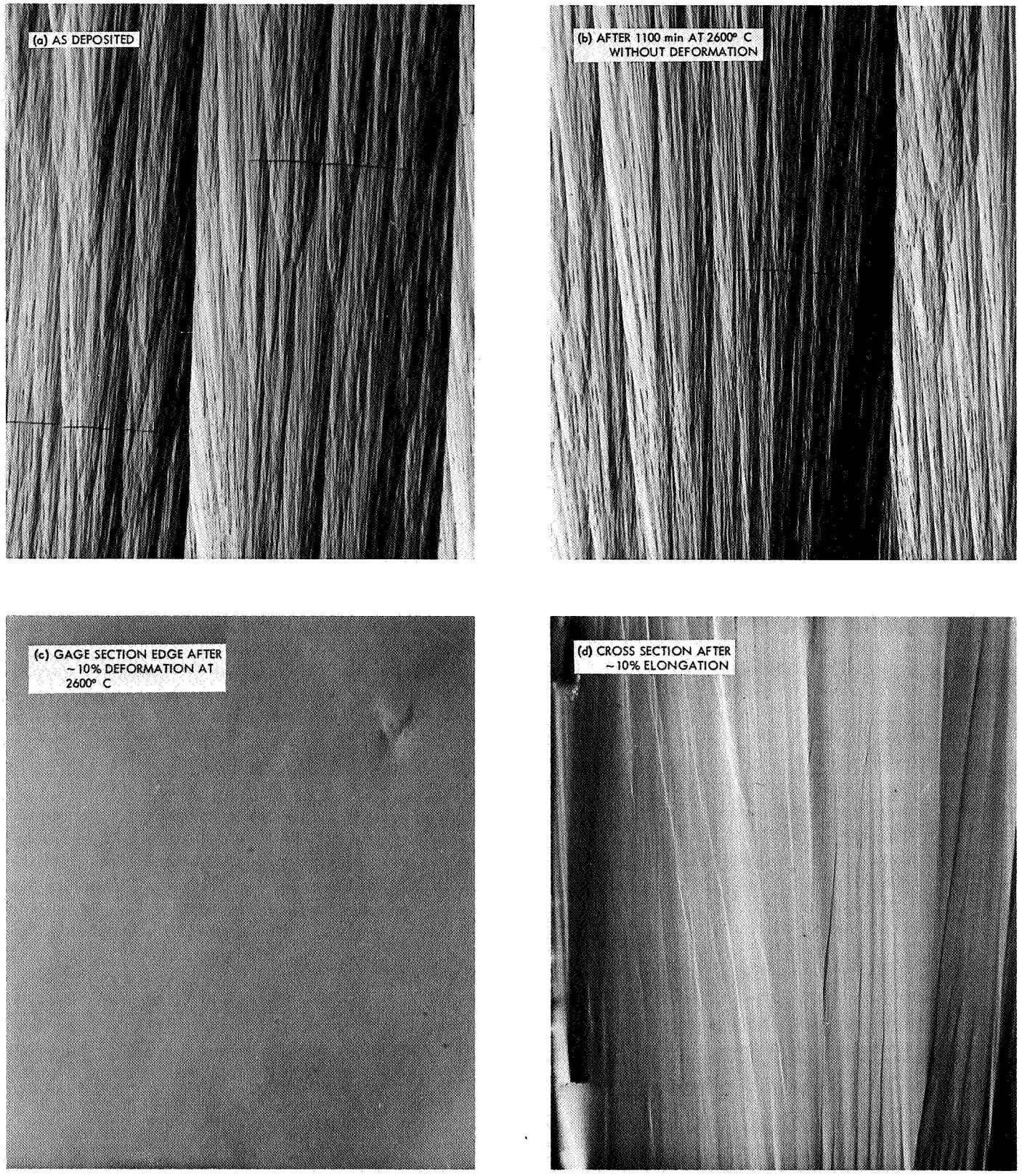

Fig. 1. Microstructure of pyrolytic carbon normal to substrate (polarized light, 50×)

pyrometer that was focused on the back of the specimen-gage section and continuously recorded. Actual temperatures were determined by means of a calibrated, disappearing-filament, optical pyrometer that focused on the front surface of the specimen. Temperatures were measured on the layer-plane edge surfaces. Corrections were made for window adsorption, but no emissivity correction was applied because blackbody conditions prevailed within the precision limits to which the temperature could be measured. The temperature was found to be uniform within 10–15°C over the gage section, but fell off rapidly in the throat and grip regions.

Using an external strain-gage extensometer coupled to the grips through ⅛-in.-diameter graphite rods, specimen elongation was sensed by measuring the change in grip separation. Elongation and load were recorded on a two-pen potentiometric recorder. The system was calibrated for a constant full-scale sensitivity of approximately 10% elongation and 20,000-psi stress. When values exceeded these limits, the recorder pen was returned down-scale, using preset potentiometric zero shifters. By using this method, the data were recorded at constant sensitivity over the whole range of elongation and stress values used.

Absolute uniform-gage strains could not be determined directly from the recorded elongation for several reasons. Because of differences in the thermal expansion of the PC specimen and the graphite extensometer rods, there was an apparent specimen contraction during heat-up and an apparent expansion during cool-down. This was difficult to correct for, because the preferred-orientation texture (and thus the expansion coefficient of the specimen) changed as a function of heat treatment and deformation. Some irreversible elongation also occurred under no load, because of partial dewrinkling caused by annealing of the as-deposited material at the higher temperatures. In addition to the uniform-gage strain, the recorded elongation also included contributions from deformation of the throat and grip portions of the specimen, and from the grips themselves. Finally, there was a possibility of small contributions from slight changes in alignment when the load was applied or removed.

To determine with precision the actual plastic, uniform-gage elongation, and to calibrate the recorded elongation response, a pattern of fiducial lines was drawn on each specimen by using an acetate drafting ink. Clearly distinguishable against the dark gray of the specimen, these black-ink lines survived temperatures up to at least 2900°C and elongations on the order of 30%. By measuring the positions of the lines with a traveling-micrometer microscope, not only the gage elongation, but the distribution of deformation along the entire length of the specimen, were determined. As shown in Fig. 2a and b, the strain distribution agreed closely with that expected from the specimen shape.

Measurements of a number of specimens, and over a wide strain range, disclosed that the recorded elongation agreed favorably with the actual elongation of the portion of the specimen between the grips (this included the throat regions as well as the gage section). The uniform-gage elongation was found to be about two-thirds of the recorded elongation. The recorded creep rates $\dot{\epsilon}$ and creep strains ϵ_c reported herein can be converted to approximate absolute values by multiplying by this factor. Contributions from grip deformation amounted to no more than a few tenths of a percent; and, with the possible exception of the small instantaneous elastic strains, alignment-change effects were negligible.

In the initial creep experiments, especially at temperatures of 2700°C and above, some difficulty was experienced with deposition of carbon evaporated from the heating element. An adherent deposit built up on the gage-section edges, partially obscuring the ink lines and, because of differential thermal expression stresses, causing kink deformation of the specimen corners during cool-down (Ref. 19). Although this deposit appeared to have no serious effect upon the results, it was bothersome. In later experiments, deposition on the specimen was prevented by wrapping shields of flexible graphite foil around the gage section or the grips, and tying the shields in place with carbon yarn.

III. Results

Using the ink fiducial-mark technique, a feature of the deformation was observed that apparently was not reported before. Over the initial 10% or so of recorded elongation (stage I), the strain distribution determined on the two-layer plane edge and the two-layer plane face surfaces of the specimen were in very good agreement, as shown in Fig. 2b. With further deformation (stage II), data from the two-layer edge surfaces continued to follow the expected distribution, but strong anomalies generally developed in the layer-face surface data.

The uniform-gage elongations were lower than expected, and large local strains occurred in the throat

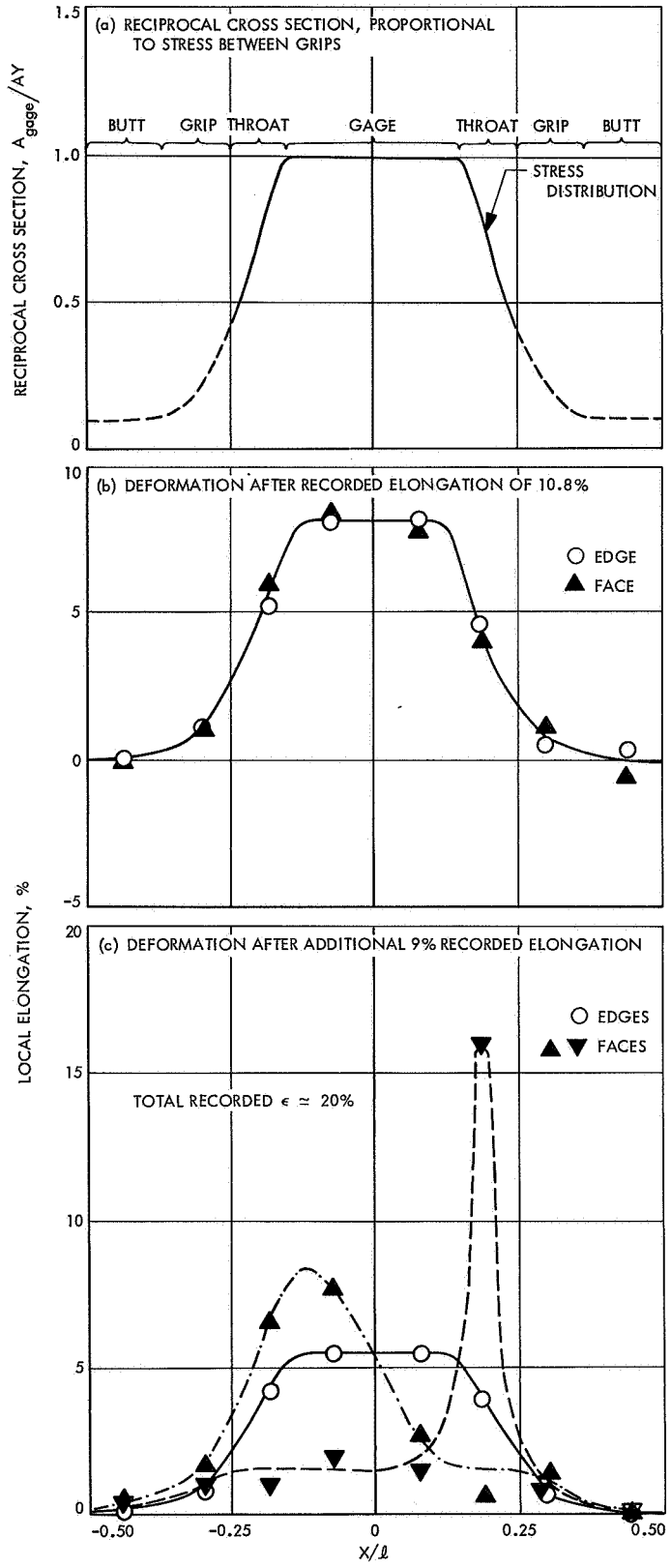

Fig. 2. Distribution of stress and elongation in specimen as function of distance from center in units of total length

regions, as shown in Fig. 2c. Further investigation confirmed that thin layers ($\leqslant$0.005 in. thick) on the layer-plane faces had failed in the throat regions, and were no longer fully supporting the load. The ends of the edge-surface ink lines, adjacent to the faces, were sheared, and fresh shear surfaces or fine cracks could often be found in the throat portions of the layer faces.

Usually, these failures occurred on opposite faces and at opposite ends of the specimen. The reason for this behavior is not entirely understood. It could result, in part, from slight misalignment of the specimen in the grips; the temperature gradient in the throat region could also play a role. The general occurrence and reproducibility of the major features of this effect suggest, however, that it is related, in some more fundamental way, to the structure or other intrinsic characteristics of the specimens themselves. It did not appear to be peculiar to the particular lot of PC or to the deformation procedures used in this study. Reexamination of specimens from other lots of PC that were deformed under different detailed conditions in earlier investigations produced evidence of similar phenomena. Primarily because of the thinness of the failed layers, the influence of this effect upon the other observations made in this investigation did not appear to be serious.

Reduction in area (RA), measured at the center of the uniform-gage section, is plotted in Fig. 3 as a function

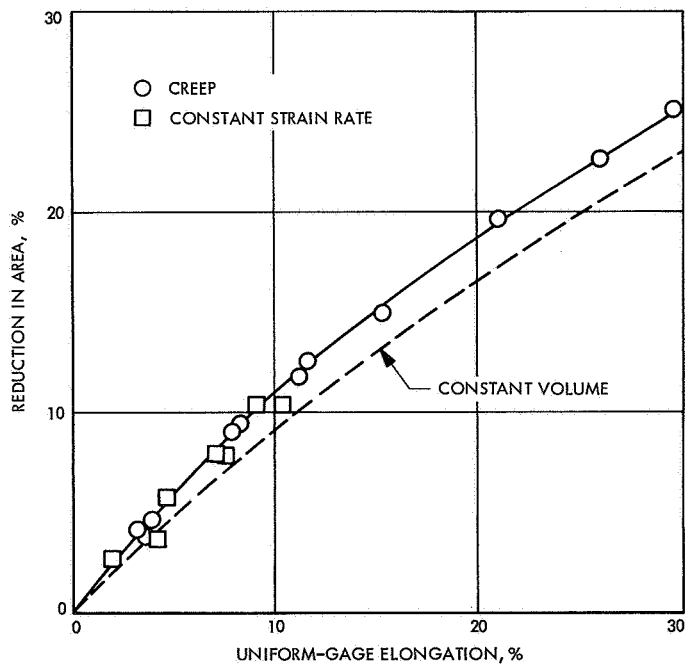

Fig. 3. Reduction in gage cross-section area as a function of gage elongation

of uniform-gage elongation determined by using ink fiducial marks. Data obtained on creep specimens are identified by the circles, data for several specimens of the same carbon, which were deformed at a constant cross-head rate equivalent to a strain rate of about 2×10^{-4} s^{-1}, are identified by the squares. Over the entire elongation range investigated, the observed RA exceeded the theoretical constant-volume value. The excess RA developed gradually during the initial 4–8% of elongation. Thereafter, the experimental results paralleled the theoretical curve with a constant offset of about 2% RA. This shows that necking did not contribute to the excess RA (no evidence for necking has been observed in any of the tensile-deformation investigations of PC carried out at JPL).

During the initial stages of the deformation, then, the gage-section volume decreased (the density increased) by about 2%; however, from about 8% to at least 30% of uniform-gage elongation, the deformation occurred at constant volume. The initial macroscopic-volume decrease can be entirely accounted for by the decrease in crystallographic unit-cell volume, which is attributed to the graphitization that occurs during stage I deformation of as-deposited PC (see Ref. 3). A decrease of about 2% in the mean interlayer spacing (from about 3.43 to $\leqslant$3.36 Å), with no change in spacing within the layer plane, is associated with the graphitization transformation.

The surface-failure phenomenon described above could have influenced these results, making the observed RA *smaller* than it would have been had the gage section deformed entirely homogeneously. Within the probable error of the measurements, any effect would be small, however, because the surface failure was observed only after the graphitization process was essentially complete, and only a small fraction of the cross section was affected because the failed layers were very thin.

In examining creep behavior, it is convenient to plot the logarithm of creep rate $\dot{\epsilon}$ as a function of the logarithm of creep strain ϵ_c. Creep strain is the time-dependent portion of the recorded strain, which is defined as the difference between the total recorded strain and the instantaneous recorded strain that occurs when the load is applied or changed. Comparison of the effects of positive and negative load increments showed that the instantaneous strain was largely elastic; thus, the creep strain is the plastic component of the total recorded strain. In common with the behavior of other types of carbon and graphite, the creep rate of PC decreases monotonically with increasing strain over most of the deformation range investigated. In the as-deposited PC used in this study, however, there was an anomaly in the creep-rate/strain relationship in the early stages of the deformation. As shown in Fig. 4, in the range

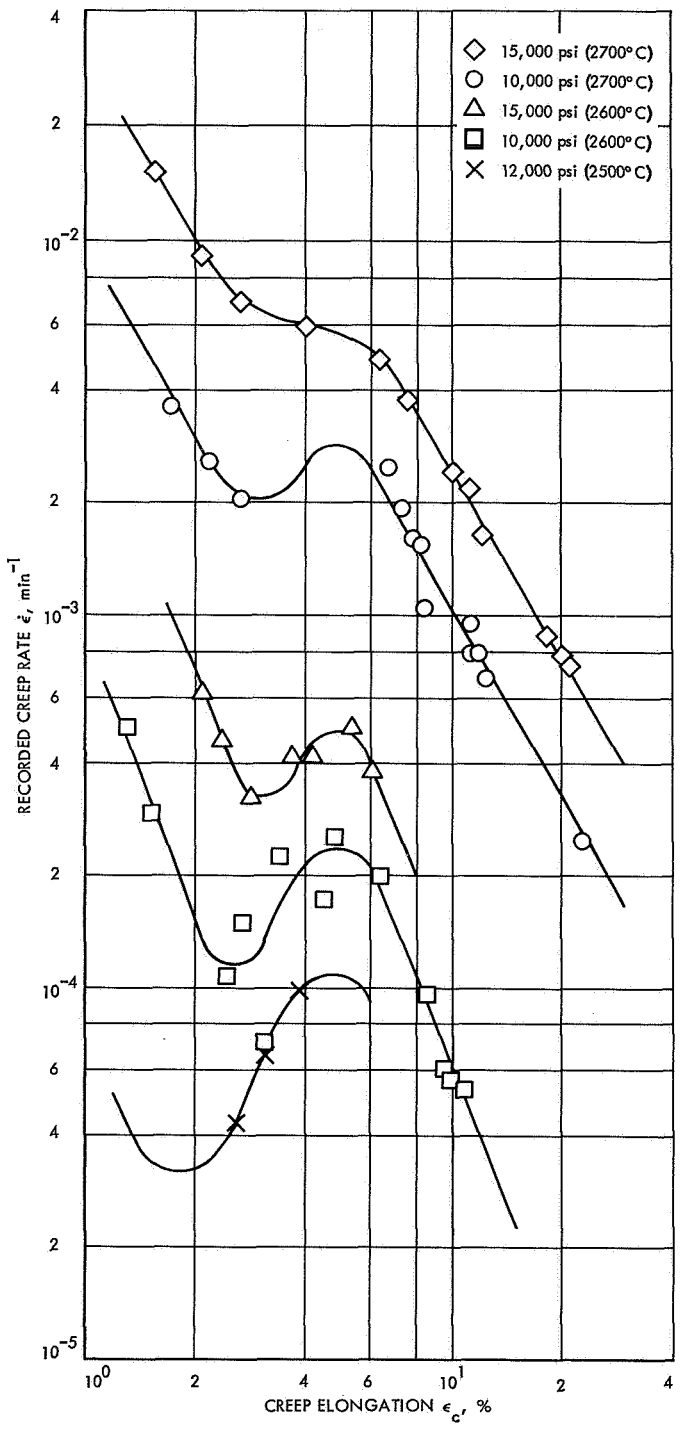

Fig. 4. Dependence of recorded creep rate on recorded creep strain at representative temperatures and stresses

$2.5 < \epsilon < 7\%$, the creep rate increased by as much as an order of magnitude (based on extrapolation of the curves at $\epsilon_c < 2.5$ and $\epsilon_c > 7\%$).

The data shown are representative of the forms the anomaly can take. At low temperatures or low stress levels, a local minimum is followed by a local maximum. At high temperatures or high stress levels, the anomaly tends to deteriorate to a plateau or to an inflection point. Although only a few representative curves are shown for clarity in Fig. 4, this behavior was observed in all of the specimens tested. It indicates that beginning after about 2–3% recorded creep elongation (1.3–2% uniform-gage elongation), a change in deformation mechanism or mode occurs; beyond about 8% creep elongation (5% uniform-gage elongation), the deformation continues via the new mechanism alone. Evidently this change in mode accompanies the dewrinkling and graphitization that occur during stage I deformation.

The belief that creep rate depends upon structure and that structure changes during creep deformation is generally accepted. To be meaningful, the dependence of creep rate on stress (or temperature) must be determined under conditions in which the structure is the same. The steady-state creep rate is often used for such determinations. With the exception of the anomaly in the early stages of deformation, however, the creep rate of PC decreases steadily as creep proceeds, and no steady-state region exists. If it is assumed that the dependence of creep rate upon structure is a function only of creep strain, then creep rates at the same strain could be compared for different specimens tested at different stress levels. Variation in the behavior of nominally identical specimens of the same material is well known, however, especially in the high-temperature testing of carbons and graphites.

These difficulties can be avoided by using a stress-change technique. After a sample has crept for some time under stress σ_1, the stress level is suddenly changed to σ_2 (which may be either larger or smaller than σ_1), and a new creep rate is established, as is illustrated by a portion of an actual PC creep curve in Fig. 5. If no transient behavior accompanies the stress change, the creep rates $\dot{\epsilon}_1$ and $\dot{\epsilon}_2$ that were observed immediately before and after the change from σ_1 to σ_2 may be used to calculate the stress dependence. As shown in Fig. 5, however, an appreciable transient response was observed. Immediately after a stress increase, the creep rate was abnormally high; immediately after a stress decrease, the

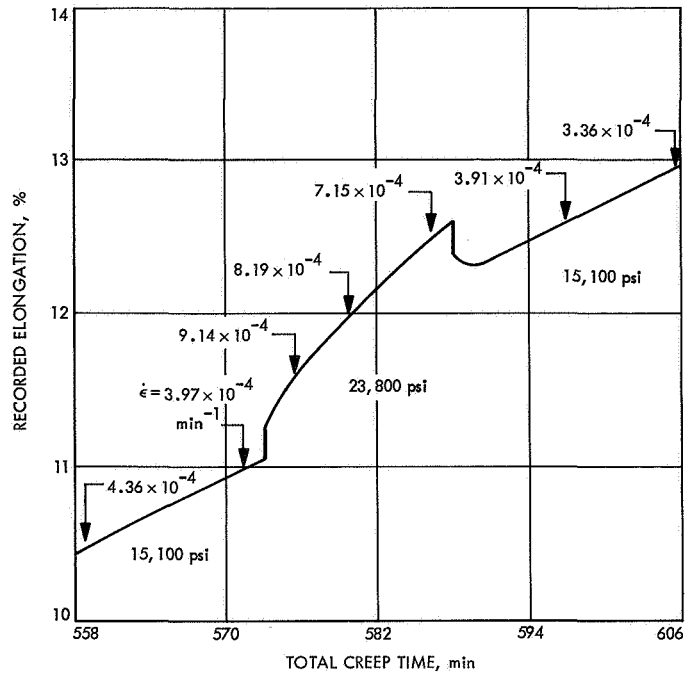

Fig. 5. Portion of a typical creep curve showing stress changes and creep-rate values (2600°C)

rate was negative, and passed through zero before assuming the normal value. The magnitude of these transient responses, and the time required for them to die out, varied with the temperature and the size of the stress increment. In general, the time was short, but sufficient for a significant decrease in creep rate to have occurred under constant stress conditions.

Some analytical technique is required, therefore, to distinguish the normal creep rate from the transient response, and to extrapolate creep rates at different stress levels to the same strain value. It was found that the logarithm of the creep rate was an approximately linear function of the logarithm of the creep strain for $\epsilon_c > 7\%$. By periodically changing the stress among a range of values over the course of an isothermal creep test, and by plotting the results in this way, the creep behavior over a broad range of stress and strain can be obtained on a single specimen, as shown in Fig. 6. The numbers in parentheses indicate the order in which the stress changes were made. Obviously transient creep rates were not plotted. At constant temperature, creep rates obtained under the same stress fall on the same line (within experimental scatter) regardless of whether the stress had been increased or decreased, and all of the lines are parallel. These characteristics of the results justify the conclusion that this method of analysis gives the proper, normal creep rates for each stress level.

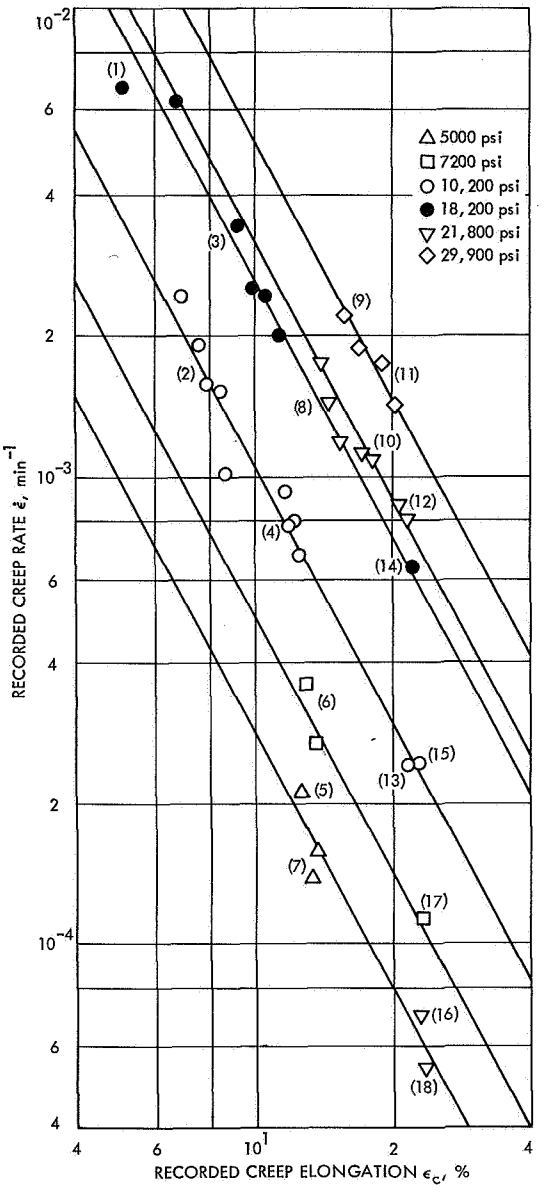

Fig. 6. Recorded creep rate as a function of recorded creep elongation at several stress levels on a single specimen at 2700°C

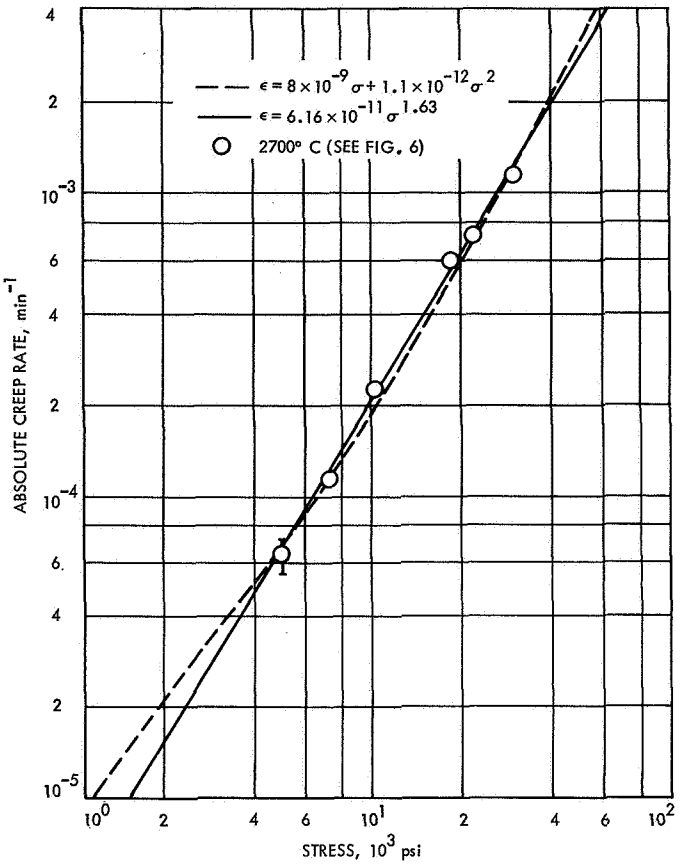

Fig. 7. Recorded creep rate as a function of stress at $\epsilon_c \sim 25\%$

When the data have been put into the form of Fig. 6, Eq. (1) can be applied to determine the stress exponent n. A vertical slice is made through the log $\dot{\epsilon}$ vs log ϵ_c plot at some value of ϵ_c, and log $\dot{\epsilon}$ is then plotted as a function of log σ. As shown by the solid curve in Fig. 7, a good linear relationship is found, indicating that n is not a function of the stress and that Eq. (1) is an appropriate expression of stress dependence. The significance of the dashed curve is discussed below. Stress exponent n is represented by the slope of the straight line, as in

$$n = \left[\frac{d \log \dot{\epsilon}}{d \log \sigma}\right]_{\epsilon_c} \tag{2}$$

Because the lines in Fig. 6 are parallel, the value of ϵ_c is not important; however, it is prudent to choose an ϵ_c that requires minimum extrapolation. The graphical technique of Fig. 7 was used to calculate n when data were obtained at several stress levels. In many tests, only two or three stress levels were used, wherein n was calculated by direct application of Eq. (1) to data for pairs of stresses. To determine the proper strain-rate values, however, the data were still analyzed as in Fig. 6.

All of the n values determined in this investigation are plotted in Fig. 8 as a function of creep elongation. Each symbol shape represents a separate specimen, and the shading indicates the temperature range. Initially, the stress-dependence is high, when $n \simeq 4$. However, n decreases very rapidly with increasing strain, and levels out at a constant value of 1.5 ± 0.4 for all $\epsilon_c > 5\%$. The strain-independence of n in stage II deformation is, of

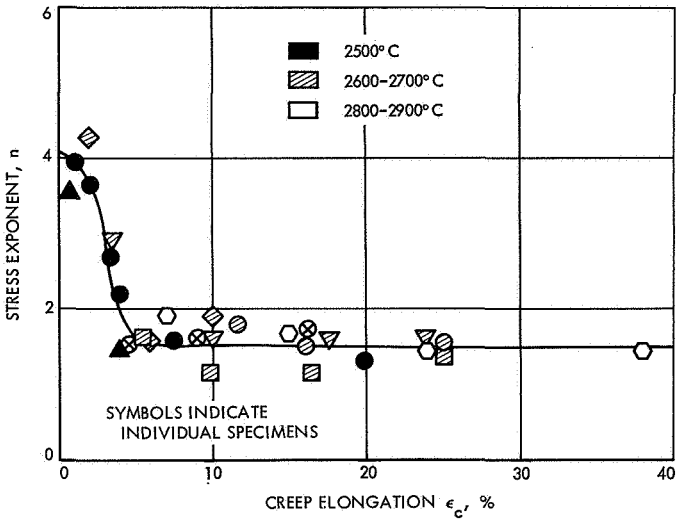

Fig. 8. Stress exponent *n* as a function of recorded creep elongation for various specimens in various temperature ranges

course, expected from the parallelism of the lines in Fig. 6. The value of n also appeared to be independent of temperature in stage II. At low strain values, insufficient data were obtained to determine whether n was independent of stress and temperature in the earliest stages of the deformation. In the region of the creep-rate anomaly, however, the dependence of the shape of the log $\dot{\epsilon}$ vs log ϵ_c curve on temperature and stress (see Fig. 4) indicates that creep behavior is probably not characterized by unique n values in this transition range.

The decrease in creep rate with increasing creep strain for $\epsilon_c > 5\%$ can be described in terms of a progressive hardening of the material as the deformation progresses. This is analogous to the concept of work hardening in the stress–strain behavior of metals. The slope of the log $\dot{\epsilon}$ vs log ϵ_c plots

$$h = \left[\frac{d \log \dot{\epsilon}}{d \log \epsilon_c}\right]_T$$

is a convenient measure of the creep-hardening rate. When defined in this way, h is independent of both stress and strain ($\epsilon_c > 7\%$) in PC because the plots for different stresses are linear and parallel within experimental scatter. Consistently, however, h was observed to be an inverse function of the temperature.

To verify this, a special creep test was run at a constant load (stress level about 15,000 psi), and the temperature was periodically increased and decreased over the range 2500–2900°C. As shown in Fig. 9, the results were analyzed in exactly the same way as were the stress-change data. The regular decrease of h (numbers in parentheses) with increasing temperature is apparent. A plot of h as a function of temperature is shown in Fig. 10. Squares represent the data from Fig. 9, and the circles represent average values determined from a number of other tests in which the primary objective was investigation of the stress dependence of ϵ. The two sets of results are in general agreement.

An effective creep-activation energy can be calculated from data such as those in Fig. 9. Because h varies with temperature, the activation energy will be a function of the creep strain. Using the data of Fig. 9, activation-energy values of 216, 250, and 285 kcal/mole were calculated at creep-strain levels of 8, 16, and 40%, respectively.

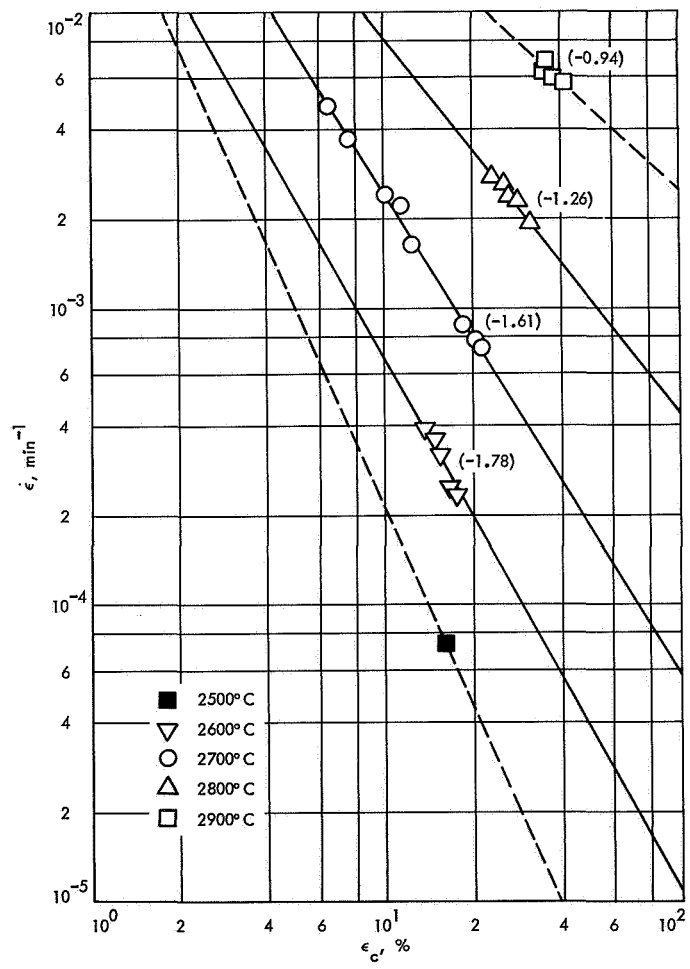

Fig. 9. Recorded creep rate as a function of recorded creep elongation at various temperatures at a stress of ~15,000 psi on a single specimen

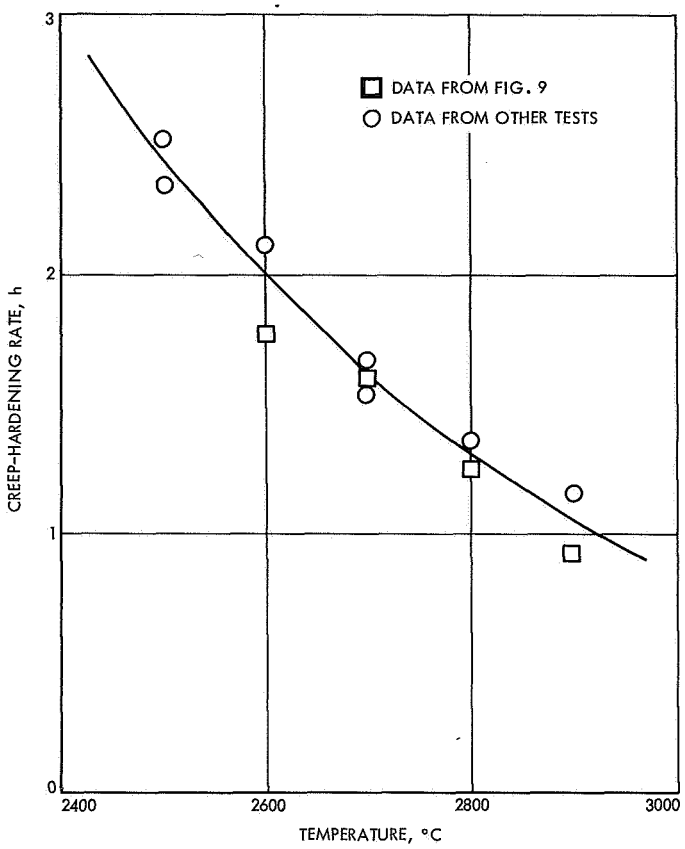

Fig. 10. Creep hardening rate *h* as a function of temperature

More limited temperature-change tests (over a range of 100–200°C), performed in conjunction with several of the stress-dependence tests, gave ΔH values ranging from 240 to 260 kcal/mole in the creep-strain range 15–27%. Although no correlation with strain was apparent in these data, the values are in general agreement with those calculated from Fig. 9.

In general, a large time- and temperature-dependent strain recovery occurs in carbons and graphites when the creep load is removed. In binder–filler graphites (see Refs. 11 and 18) and in glassy carbon (see Ref. 13), 25% or more of the total creep strain is recoverable in time (under no load) at the creep temperature, and the recovery rate increases with temperature. The negative creep rates following stress reduction (see Fig. 5) indicate that some recovery also occurs in PC, but earlier unpublished observations at JPL indicated that the effect was much smaller than in other carbons and graphites.

Although no systematic study of creep recovery was made in this investigation, the study confirmed that the amount of creep recovery is small, especially in well-graphitized, highly oriented PC. Representative data for several specimens are listed in Table 1. Despite the relatively short recovery times, when allowance is made for the probable temperature dependence of the recovery rate, it is apparent that significant recovery may occur during stage I; after large stage II elongations, however, the proportion of recoverable creep strain is relatively small.

The size of the instantaneous strain increments associated with both positive and negative stress changes was also observed to decrease with increasing creep strain, especially during stage I. The data indicate an increase in Young's modulus by more than a factor of 5 (from <1 to $\sim 5 \times 10^6$ psi) over the first 10% of elongation. Similar results were obtained from constant cross-head-rate tensile tests (Ref. 20).

Because of the increase in preferred orientation texture, a significant increase (already observed at room temperature when hot-worked specimens were used, as cited in Refs. 21–23) is anticipated in tensile modulus parallel to the substrate.

Table 1. Creep recovery behavior of pyrolytic carbon

Temperature, °C	Stress, 10^3 psi	Recorded creep strain, %	Recovery time, min	Recorded recovery strain, %	Proportion of total strain recovered, %
2500	10	3.9	9	0.3	8
2500	12	4.3	35	0.6	14
2700	10	19	27	0.6	3
2700	5	25	15	0.25	1
2800	10	39	15	0.4	1

The apparent modulus values observed herein were as much as an order of magnitude smaller than expected from the room-temperature values. This disparity could be attributed, in part, to the decrease in modulus with temperature, which is characteristic of crystalline solids, and has been observed in undeformed PC (Ref. 24). However, it is unlikely that the negative temperature-dependence can account for a decrease by more than a factor of 2–3. A significant part of the small elastic strain observed was probably induced by the grips and by other sources of systematic error. Nevertheless, the consistent trend of decreasing instantaneous strain with

elongation cannot be explained on this basis, and probably had its origin in an actual (and expected) modulus increase.

IV. Discussion

The creep-rate anomaly observed herein during the initial 3–5% of recorded elongation has apparently not been reported before. Obviously, the failure of thin, basal-plane surface layers near the end of stage I deformation could contribute to this anomaly. Although these failures were observed only after >10% recorded elongation, it is possible that they were initiated earlier, but the precision of the deformation–distribution analysis was not sufficient to detect them immediately. These surface failures, however, reduced the effective cross section by only about 10%, at most. Even with the maximum observed stress exponent value of 4, this would produce a strain-rate increase of less than a factor of 2, as compared with the observed order-of-magnitude increase; therefore, some other explanation is required.

It is significant that the $\dot{\epsilon}$ anomaly was not observed by Kotlensky (see Ref. 15), who also investigated PC creep in the range below 10% elongation. It is possible that this behavior is peculiar to the particular PC material used in this study. This is unlikely, however, because the preparation and structure of the as-deposited material was not unusual in any way; also, the structural changes associated with heat treatment and deformation (see Fig. 1 and Refs. 3 and 5) were typical of those observed earlier for a number of other substrate-nucleated PCs (Refs. 1, 2, 15, and 25).

Kotlensky used an analysis method that was not as sensitive to fluctuations in creep rate as the method used in this study, and it is possible that the anomaly occurred but was overlooked. It seems more likely, however, that the different behavior derived from the fact that samples were tested in the as-deposited condition in this study, whereas Kotlensky annealed his PC for ½ h at 2800°C before testing.

This pretreatment produced significant changes in the structure of the carbon. A substantial graphitization and increase in preferred orientation occurred. The interlayer spacing decreased from 3.43 to 3.38 Å, and the rms layer plane misorientation angle (Ref. 26), relative to the substrate, decreased from 19 to 13.5 deg. These structural changes, which occur spontaneously during annealing (see Ref. 25), are greatly accelerated by deformation, with the preferred orientation (in particular) being dependent upon the strain (see Refs. 2 and 3). It is likely, therefore, that the $\dot{\epsilon}$ anomaly results from a real change in deformation mechanism associated with the change in structure.

This interpretation is strongly supported by the decrease in the stress-dependence exponent from an initial value of ~4 to ~1.5 during the initial 5% of creep elongation (see Fig. 8). For dislocation climb, $n \geq 4$ is expected (Refs. 27 and 28), whereas the value of $n = 1.5$ is close to that for viscous processes ($n = 1$). The as-deposited PC had a typical substrate-nucleated, growth-cone structure (see Fig. 1a). Within the primary cones, which are separated by relatively high-angle boundaries, there is an extensive subcone structure with a high density of low-angle tilt and twist boundaries. The initial changes produced by heat treatment and deformation involve this substructure. It is reasonable to assume that this initial breakdown of the as-deposited structure, involving the removal of substructure boundaries, would require dislocation–climb processes. Once the breakdown of the structure has been initiated, however, in the earliest stages of the deformation, the rate-determining process evidently changes very rapidly to some mechanism other than dislocation climb, and the deformation proceeds more easily.

The monotonic decrease in creep rate and the constant stress-exponent value for all recorded strain levels above about 5% (about 3% uniform-gage elongation) indicate that a single mechanism (or specific combination of mechanisms) dominates the subsequent deformation behavior. The low n value suggests that the principal mechanism is a viscous one. The excess of n over unity could be a result of experimental error, or it might indicate the simultaneous operation of a viscous process and some other secondary mechanism with a higher n value. The fact that n is independent of stress over the range investigated, however, places a constraint on the n value that such a secondary mechanism could have. In Fig. 7, the dashed line shows that the observed data are consistent with a stress-dependence of the form

$$\dot{\epsilon} = A\sigma^{n(1)} + B\sigma^{n(2)} \tag{3}$$

where

$$n(1) = 1$$

$$n(2) = 2$$

Values of $n(2) \geq 3$ would, however, result in strong curvature of the log $\dot{\epsilon}$ vs log σ plot, which is inconsistent with the data.

Having thus established the possibility of a secondary mechanism with $n < 3$, the remaining discussion will proceed on the assumption that the primary deformation mechanism is viscous. Further discussion of the detailed mechanism of any secondary process (or a single primary process with n equal to 1.5) that may be involved does not appear to be warranted by the precision of the present data and the very limited, current understanding of high-temperature dislocation behavior in graphite.

Other important characteristics of the deformation include the temperature-dependence of the creep rate, as well as the progressive hardening and its apparent temperature-dependence. Hardening appears to be characteristic of the high-temperature, creep-deformation behavior of all types of carbon and graphite; therefore, it does not provide much specific information on the deformation mechanism of highly oriented, well-graphitized PC. Nevertheless, the hardening is significant because of its universality. Hardening may result from depletion of the defects, such as glissile dislocations, which provide plasticity, or from the creation of barriers to the deformation as the strain increases. The initial deformation properties of materials may often be recovered by annealing at high temperatures, especially when hardening is of the second type.

The high-temperature creep behavior of crystalline solids generally results from the simultaneous occurrence of hardening and recovery. When recovery just balances hardening, steady-state creep occurs. If the hardening rate exceeds the recovery rate, the creep rate continually decreases.

The temperature-dependence of the hardening rate observed herein suggests that this may apply to PC, with a temperature-dependent recovery rate. It is possible, however, that this temperature-dependence could be merely an experimental artifact. Because of the very strong temperature-dependence of graphite creep, as is discussed below, an apparent decrease in hardening rate (with increasing temperature) could be induced by an undetected upward drift in temperature during the experiment. Failure to detect temperature drift could be attributed to progressive clouding of the view port (window) as the temperature increased. Pre- and post-test transmission measurements indicated that the resultant temperature error was small (although perhaps not negligible). More significantly, an investigation of the creep behavior of glassy carbon, using the same equipment and techniques, disclosed no temperature-dependence of the hardening rate of glassy carbon (see Ref. 13). This disclosure suggests that the temperature-dependence observed in PC is probably real; however, the evidence is not conclusive.

The average, effective activation-energy value ΔH, determined herein for creep of PC, is 250 ± 40 kcal/mole. This includes the range of values determined at strain levels of 8–40% from the data in Fig. 9. If these results were ignored, the scatter band would be reduced to ± 15 kcal/mole. As noted in Ref. 11, a temperature error of $\pm 10°C$ can change the apparent activation-energy value by ± 30 kcal/mole; thus, the range of observed values can reasonably be attributed to experimental error. Because the apparent strain-dependence of ΔH results from the temperature-dependence of the hardening rate, it could also be attributed to temperature errors of this magnitude (as discussed above).

The activation energies found herein agree very well with the creep ΔH values for PC as determined by Kotlensky (see Ref. 15), and for stress-recrystallized, binder–filler graphite (ZTA) established by Zukas and Green (see Ref. 11). These activation energies also agree with the ΔH values for structural transformation and graphitization in PC (Refs. 25 and 29), as well as for graphitization in conventional petroleum and pitch–coke carbons (Ref. 30). The existence of a common ΔH value of approximately 250 kcal/mole for a variety of high-temperature processes in a variety of types of graphitizing carbons and graphites points to the existence of a common rate-limiting, thermally activated process.

The most likely candidate for such a process is self-diffusion mass transport. Although self-diffusion in graphite is still not understood in any detail, abundant theoretical and experimental evidence, reviewed elsewhere (see Refs. 5 and 25), indicates that diffusion by a defect mechanism occurs with an activation energy in the range 200–300 kcal/mole. The most extensive evidence relates to diffusion by a vacancy mechanism within the layer planes. However, as recently shown (Refs. 31 and 32), diffusion normal to the layers induced by an interstitial mechanism may also occur with a similar activation energy.

In general, dislocation–glide processes, often thermally activated, dominate the deformation behavior of crystalline solids. The difficulties encountered in explaining the plasticity of graphite by dislocation glide have, however, already been reviewed elsewhere (see Refs. 1 and 5), as

well as in the introduction to this report. Although it would be premature to rule out the possibility of non-basal dislocation glide in graphite, there is little evidence (to date) that it plays an important role. The absence of effective dislocation–glide mechanisms is one of the criteria (Ref. 33) favoring deformation by a diffusion mass-transport process of the type proposed independently by Nabarro (Ref. 34) and Herring (Ref. 35).

Jenkins and Williams (Ref. 36) have suggested that this is the dominant high-temperature creep mechanism in graphites. In its simplest form, plastic strain is produced (in response to an applied stress) by the diffusional transfer of material from the compression to the tension faces of individual crystallites. The creep rate is given by

$$\dot{\epsilon} = \frac{AD\sigma}{L^2T} \tag{4}$$

where

A = a constant

D = appropriate diffusion coefficient

σ = stress

L = crystallite diameter

T = absolute temperature

Nabarro–Herring creep is thermally activated with the diffusion-activation energy; in some cases, however, grain-boundary diffusion, rather than lattice diffusion, may be involved. The inverse T dependence can be neglected when ΔH is large, and the creep rate is proportional to the first power of the stress. These properties are in agreement with the behavior observed herein. If c-axis diffusion can occur (see Ref. 5), the gage-section, dimensional-change characteristics of PC also are consistent with diffusional creep. The hardening could be accounted for by crystallite growth.

Evidence (Refs. 3, 37, and 38) exists that the spontaneous increase in apparent crystallite size and perfection that occurs on annealing PC is greatly accelerated and extended by appropriate deformation (tension parallel or compression normal to the layers). A negative temperature-dependence of the hardening rate would not, however, be expected with this mechanism. Without more detailed knowledge of D and L than is now available, it is not possible to show conclusively that this mechanism could account for the observed creep rates; however, rough order-of-magnitude arguments can be advanced to show that such a mechanism is feasible (see Refs. 1, 4, and 5).

Friedel suggests that diffusional creep can occur with point-defect sources and sinks other than crystallite boundaries (Ref. 39), and Jenkins has suggested that unit c-axis edge dislocations in the basal planes could be involved (Ref. 40). It is not clear, however, that the characteristics of such a process would necessarily be the same as for crystallite boundary sources and sinks. For example, Nabarro (Ref. 41) has described a steady-state, diffusional-creep mechanism that involves dislocations in which the creep rate depends upon the third or fifth power of the stress, depending upon whether the diffusion path is through the bulk crystal or along dislocation cores.

Another possible deformation mechanism, peculiar to highly oriented layer-structure materials, that should be considered is the pulling apart of interleaved packets of fractured, or otherwise discontinuous, layer planes (see Refs. 1 and 2). It was observed that the outer layers of the specimen failed near the end of the first stage of deformation, and were thereafter coupled to the applied stress only through shear forces. If a similar phenomenon occurred generally throughout the cross section, with the ends of the discontinuous layer-plane packets distributed randomly along the length of the gage section, tensile deformation could proceed in a pure shear mode as the layer packets slipped apart. The shear flow stress has been shown to be thermally activated with $\Delta H \simeq 250$ kcal/mole, but the stress levels are quite low (Refs. 1 and 42–44). To account for the observed high tensile flow and fracture stresses, it is necessary only to assume that many thin ($< 10^{-3}$-in.) layer packets shear in parallel.

A careful microscopic examination of the edges of the ink-line marks on the gage section disclosed no evidence of this type of deformation; this may, however, indicate only that the layer-packet thickness is substantially less than this estimated maximum value. To maintain constant density, it is necessary to assume that, as the packets pull apart, the resulting interlaminar cracks collapse and heal completely; this implies very thin layers. Use of this simple mechanism would induce a decrease in thickness at about twice the observed rate and no decrease in width. This difficulty can be resolved by recalling the instability of thin sheets that develop wrinkles and corrugations parallel to the stress axis when deformed in tension. Because the weak van der Waal's bonding between the layers in graphite may be further

attenuated by thermal expansion and agitation at high temperatures, the layer planes may behave as individual or loosely coupled thin sheets (see Ref. 40). In this way, the excessive decrease in thickness could be converted into an appropriate width decrease. Such corrugations are, in fact, observed in the structure of tensile-deformed PC (see Refs. 1, 15, and 40), but they have generally been regarded as a residue of the initial cone structure.

Several other characteristics of this model, however, fail to agree substantially with the observations. The stress exponent value for basal-plane shear was found to be $n = 3$ (see Refs. 1 and 43). Furthermore, at high temperatures and in well-oriented graphite, basal-plane shear exhibits little or no strain hardening (see Refs. 1, 42, and 44). Apparently, there is no simple way to account for the pronounced creep-hardening observed; this, perhaps, is the most serious deficiency of this deformation mechanism.

Finally, unlike Nabarro–Herring creep, the mechanism in question would not be capable of providing plasticity in dewrinkled material under compression that is normal to the layer planes. Although little data are available on the deformation behavior under these conditions, parallel-to-layer expansions $\geq 15\%$ and normal-to-layer compressions $\geq 20\%$ have been reported for as-deposited PC (see Refs. 37 and 38). Considerably larger than the dewrinkling strains, these values indicate appreciable stage II plasticity in this mode.

Other deformation mechanisms, consistent with at least some of the observed characteristics of PC, can also be devised. One possibility, often important in other materials, is crystallite boundary sliding. A mechanism of this type, proposed by Gifkins (Refs. 45 and 46), involves small protrusions on the boundary and provides viscous, thermally activated creep rates that are appreciably larger than those provided by the usual Nabarro–Herring mechanism. Hardening could occur by reducing the number of boundaries (crystallite growth) or by increasing the length of the boundary protrusions (perhaps by coalescence). At present, no evidence that such protrusions exist on crystallite boundaries in graphite is available. In fact, there is little evidence of a well-developed grain structure in PC that is similar to that observed in metals and ceramics. Boundaries inclined to the *c*-axis would be required to account for dimensional changes in the gage section, but such boundaries have not been observed.

Jenkins (see Ref. 40) has suggested that unit *c*-axis edge dislocations could contribute directly to the plasticity within the layer planes. Such defects, either present in the as-deposited material or generated during stage I deformation (by intersection of glissile basal-plane dislocations with sessile nonbasal forest dislocations), might undergo a nonconservative, thermally activated sort of glide motion within the basal planes. Such defects could thus induce the observed gage elongation and width decrease. Such defects could not, however, account for the thickness decrease; there is, as yet, little direct evidence that they significantly affect the deformation. Various combinations of the mechanisms discussed (and others not considered) might be invoked, as well; however, there is insufficient evidence to warrant such an approach at present.

The very small creep-recovery effect in PC is interesting because of the prominence of this phenomenon in the creep behavior of most carbons and graphites. Creep recovery must result from the accumulated internal stresses that are induced by the deformation and cause a reverse creep when the load is removed. This behavior is to be expected in an intrinsically highly anisotropic material such as graphite, in which the elastic moduli (and perhaps the plasticity) depend strongly upon crystallographic orientation. Large effects would be expected, and are observed, in more or less isotropic, heterogeneous binder–filler graphites and in such isotropic carbons as glassy carbon, in which there is evidence of very strong and extensive bonding between the crystallites.

Conversely, in stage II deformation, a small recovery might be expected for a dense, homogeneous, very highly oriented graphite such as PC. The results confirm this expectation.

The limited data obtained herein are also consistent with a significant decrease in recovery that is associated with the pronounced increase in preferred-orientation texture that occurs during stage I deformation. The actual amount of strain recovered is so small, however, and varies so little with total strain (at the same stress level) that a significant portion of the observed effect may be instrumental in origin, although no specific source is apparent for this. It may seem surprising that the creep-recovery behavior of ZTA—a dense, highly oriented, stress-recrystallized synthetic graphite—is reported (see Ref. 11) to be very similar to the behavior of glassy carbon and conventional synthetic graphites ($\geq 25\%$ of the creep strain recoverable). This may be interpreted as an indication that the structural perfection

required for negligible recovery effects is quite high. Although ZTA is much more highly oriented and homogeneous than conventional binder–filler graphites, it is quite inferior to PC in these respects.

V. Summary and Conclusions

Studies of the tensile-creep behavior of as-deposited PC (parallel to the substrate) have confirmed the two-stage deformation behavior of these materials, and provide new insights into the nature of the deformation processes. Early in the deformation, after about 1–2% uniform-gage elongation, an anomaly in the creep-rate vs creep-strain curve signals a change in the deformation mechanism. In the same strain range, the stress exponent n drops from its initial value of about 4 to about 1.5. Initially, breakdown of the as-deposited growth-cone structure (involving the migration and removal of tilt boundaries) dominates the behavior. It is reasonable to assume that dislocation glide and climb, consistent with the high n value, are required for this process. However, once this structural breakdown has been initiated, presumably at the level of the subcone boundaries, the rate-determining process rapidly changes to an approximately viscous mechanism, which continues out to at least 30% uniform-gage elongation.

Over approximately the first 8% of elongation, a number of structural changes take place. Graphitization occurs, producing a density increase of about 2%. Aside from the volume decrease associated with graphitization, the reduction in area shows that the deformation occurs at constant volume out to at least 30% strain. Over the same range, a pronounced increase in preferred-orientation texture and an associated increase in Young's modulus also occur. Near the end of this range, failure of thin outer layer/plane surface layers generally occurs in the throat regions. The significance of this is not understood; because the change in effective cross section is small, however, this failure appears to have little influence on creep behavior. Beyond about 5% elongation, the creep rate decreases monotonically with strain, as in other carbons and graphites. The hardening rate is independent of both stress and strain.

Although consistent evidence exists that hardening decreases with increasing temperature, it is possible that this is an artifact resulting from temperature-measurement and temperature-control errors. Where the error band includes the possibility of some strain dependence (because of a temperature-dependent hardening rate), as well as temperature errors, the creep-activation energy is 250 $\pm$40 kcal/mole. This value closely agrees with other recent results of creep studies on both PC and ZTA, as well as graphitization-kinetics studies. Self-diffusion by a defect mechanism appears to be the rate-controlling process. The stress exponent value of 1.5, observed at all strain levels above about 3%, is independent of both stress and temperature. It suggests that the dominant deformation mechanism is approximately viscous, although a secondary mechanism with $n \sim 2$ may also contribute.

Among the several primary deformation processes considered (various dislocation mechanisms, basal-plane fracture and shear, and grain boundary sliding), the self-diffusion/mass transport (Nabarro–Herring) mechanism seems most consistent with the ensemble of characteristics observed both here and elsewhere. Definite confirmation that this mechanism is the principal source of plasticity must, however, await more complete information on the detailed microstructure and self-diffusion characteristics. Finally, the strain recovery that is a general feature of the creep behavior of most carbons and graphites was found to be very small in PC, especially after dewrinkling was completed. This small strain recovery is attributed to the very high preferred-orientation texture of this material.

References

1. Fischbach, D. B., and Kotlensky, W. V., "On the Mechanisms of High-Temperature Plastic Deformation in Pyrolytic Carbons," *Electrochem. Tech.*, Vol. 5, Nos. 5–6, pp. 207–213, May–June 1967. (Reprints available as Technical Report 32-1137. Jet Propulsion Laboratory, Pasadena, Calif.).

2. Kotlensky, W. V., and Martens, H. E., "Structural Changes Accompanying Deformation in Pyrolytic Graphite," *J. Am. Ceram. Soc.*, Vol. 48, No. 3, pp. 135–138, Mar. 1965.

3. Fischbach, D. B., "The Influence of High-Temperature Plastic Deformation on the Kinetics of Graphitization of Pyrolytic Carbons," Paper No. 24, *Conf. on Aspects foundamentaux de la carbonisation et de la graphitation*, Paris, June 26–28, 1968. (To be published in *J. Chimie Physique*.)

4. Kotlensky, W. V., "Deformation in Pyrolytic Graphite," *Trans. AIME*, Vol. 233, pp. 830–832, Apr. 1965.

5. Fischbach, D. B., *Isotropic Plasticity of Graphite*, Technical Report 32-1237. Jet Propulsion Laboratory, Pasadena, Calif., Jan. 1, 1968.

6. Thomas, J. M., et al., "Chemical Evidence for the Existence of Non-Basal Dislocations in Graphite," *Phil. Mag.*, Vol. 10, p. 325, Aug. 1964.

7. Thomas, J. M., and Roscoe, C., "Non-Basal Dislocations in Graphite," in *Chemistry and Physics of Carbon*, Vol. 3. Edited by P. L. Walker, Jr., Marcel Dekker Inc., New York, 1968.

8. Green, W. V., and Kukas, E. G., "The Stress Dependence of the Creep Rate of Two Commercial Graphites," *Electrochem. Tech.*, Vol. 5, No. 5, pp. 203–206, May–June, 1967.

9. Green, W. V., "The Stress Dependence of the Creep Rate of a Uranium-loaded Graphite," *Carbon*, Vol. 4, No. 1, pp. 81–84, Jan. 1966.

10. Zukas, E. G., and Green, W. V., "Dependence of Rate of Creep on the Orientation of the Tensile Axis for Heavily Oriented Graphite," *Nature*, Vol. 212, No. 5069, pp. 1455 and 1456, Dec. 24, 1966.

11. Zukas, E. G., and Green, W. V., "High Temperature Creep Behavior of a Highly-Oriented Polycrystalline Graphite," *Carbon*, Vol. 6, No. 1, pp. 101–110, Jan. 1968.

12. Green, W. V., et al., "A Method for Determining the Microstructural Changes in Graphite That Accompany High Temperature Deformation," *Carbon*, Vol. 5, pp. 583–586, June 1967.

13. Fischbach, D. B., *Tensile Creep Studies on Glassy Carbon*, Technical Report 32-1228. Jet Propulsion Laboratory, Pasadena, Calif., Mar. 1, 1968.

References (contd)

14. Fischbach, D. B., "Stress Dependence of Tensile Creep Rate in Carbons and Graphites," *Nature,* Vol. 217, No. 5131, pp. 840 and 841, Mar. 3, 1968.

15. Kotlensky, W. V., "Analysis of High Temperature Creep in Pyrolytic Carbon," *Carbon,* Vol. 4, No. 2, pp. 209–214, Feb. 1966. (Also available as Technical Report 32-889. Jet Propulsion Laboratory, Pasadena, Calif., Feb. 15, 1966).

16. Fischbach, D. B., "The Stress Dependence of the Tensile Creep Rate in Carbons and Graphites," Paper MI 42, presented at the Eighth Carbon Conference, Buffalo, N.Y., June 1967.

17. Kotlensky, W. V., and Martens, H. E., *Tensile Properties of Pyrolytic Graphite to 5000°F,* Technical Report 32-71. Jet Propulsion Laboratory, Pasadena, Calif., Mar. 10, 1961. (Also available in *High Temperature Materials II, AIME Met. Soc. Conference,* Vol. 18, pp. 403–418. Edited by G. M. Ault, W. F. Barclay, and H. P. Munsinger. Interscience Publications, Division of John Wiley & Sons, Inc., New York, 1963.)

18. Martens, H. E., et al., "Tensile and Creep Behavior of Graphites Above 3000°F," in *Proceedings of Fourth Conference on Carbon,* pp. 511–530. Pergamon Press, New York, 1960.

19. Fischbach, D. B., "Effect of Substrate Structure on Deposition of Evaporated Carbon," *J. Mater. Sci.,* Vol. 3. p. 559, Sept. 1968. (Also available as Technical Report 32-1309. Jet Propulsion Laboratory, Pasadena, Calif., Oct. 15, 1968.)

20. Fischbach, D. B., "Carbon and Graphite Research: High-Temperature Tensile Behavior of Pyrolytic Carbons," in *Supporting Research and Advanced Development,* Space Programs Summary 37-38, Vol. IV, pp. 58 and 59. Jet Propulsion Laboratory, Pasadena, Calif., Apr. 30, 1966.

21. Price, R. J., "Young's Modulus of Pyrolytic Carbon in Relation to Preferred Orientation," *Phil. Mag.,* Vol. 12, No. 117, p. 561, Sept. 1965.

22. Kotlensky, W. V., Titus, K. H., Jr., and Martens, H. E., "Young's Modulus of Hot Worked Pyrolytic Graphite," *Nature,* Vol. 193, No. 4820, pp. 1066 and 1067, Mar. 17, 1962.

23. Fischbach, D. B., "Carbon and Graphite: B-1. Dependence of Mechanical Properties on Microstructure," in *Supporting Research and Advanced Development,* Space Programs Summary 37-41, Vol. IV, pp. 54–57. Jet Propulsion Laboratory, Pasadena, Calif., Oct. 31, 1966.

24. Bushong, R. M., and Neel, E. A., "Properties of High Density Recrystallized Graphite," in *Proceedings of Fifth Conference on Carbon,* Vol. I, pp. 595–599. Pergamon Press, New York, 1963.

25. Fischbach, D. B., *Kinetics of Graphitization: I. The High-Temperature Structural Transformation in Pyrolytic Carbons,* Technical Report 32-532. Jet Propulsion Laboratory, Pasadena, Calif., Feb. 1, 1966.

References (contd)

26. Fischbach, D. B., "Preferred Orientation Parameters for Pyrolytic Carbons," *J. Appl. Phys.*, Vol. 37, pp. 2202 and 2203, Apr. 1966.

27. McLean, D., "The Physics of High Temperature Creep in Metals," in *Reports on Progress in Physics*, Vol. XXIX, Part I, 1966.

28. Sherby, O. D., and Burke, P. M., "Mechanical Behavior of Crystalline Solids at Elevated Temperatures," *Prog. Mater. Sci.*, Vol. 13, No. 7, July 1967.

29. Fischbach, D. B., "Kinetics of High-Temperature Structural Transformation in Pyrolytic Carbons," *Appl. Phys. Letters*, Vol. 3, pp. 168–170, Nov. 1, 1963.

30. Fischbach, D. B., "Kinetics of Graphitization of a Petroleum Coke," *Nature*, Vol. 200, No. 4913, pp. 1281–1283, Dec. 18, 1963.

31. Thrower, P. A., *The Influence of Crystal Perfection on Defect Nucleation in Graphite Irradiated at High Temperatures*, Technical Report AERE-R5665. Metallurgy Division, Atomic Energy Research Establishment, Harwell, Berkshire, England, Jan. 1968.

32. Thrower, P. A., *Thermal Annealing Studies of Irradiation Defects in Graphite and the Self-Diffusion Mechanism*, Technical Report AERE-R5666. Metallurgy Division, Atomic Energy Research Establishment, Harwell, Berkshire, England, Jan. 1968.

33. Dorn, J. E., and Mote, J. D., "Physical Aspects of Creep," in *High Temperature Structures and Materials*, pp. 95–168. Edited by Freudentahl, Boley, and Liebowitz. Pergamon Press, The MacMillan Co., New York, 1964.

34. Nabarro, F. R. N., "Deformation of Crystals by Motion of Single Ions," in *Report of Conference on Strength of Solids*, pp. 75–90. University of Bristol, England, 1948.

35. Herring, C., "Diffusional Viscosity of a Polycrystalline Solid," *J. Appl. Phys.*, Vol. 21, pp. 437–445, 1950.

36. Jenkins, G. M., and Williamson, G. K., "Deformation and Creep Mechanisms in Graphite," in *Proceedings of the Joint International Conference on Creep*, p. 49. The Institute of Mechanical Engineers, London, Aug. 1963.

37. Maire, J., et al., "Preparation et propriétés d'un pyrocarbone comprimé a haute temperature," *Carbon*, Vol. 5, No. 6, pp. 575–582, June 1967.

38. Ubbelohde, A. R., Young, D. A., and Moore, A. W., "Annealing of Pyrolytic Graphite Under Pressure," *Nature*, Vol. 198, No. 4886, p. 1192, June 22, 1963. (Also available in *Proc. Roy. Soc. Ser. A*, No. A280, pp. 153–159, June 21, 1964.)

References (contd)

39. Friedel, J., *Dislocations.* Pergamon Press, New York, 1964.

40. Jenkins, G. M., *A New Deformation Mechanism in Pyrolytic Carbon at High Temperatures,* Technical Report 32-1243. Jet Propulsion Laboratory, Pasadena, Calif., Feb. 15, 1968.

41. Nabarro, F. R. M., "Steady-State Diffusional Creep," *Phil. Mag.,* Vol. 16, No. 14, pp. 231–238, Aug. 1967.

42. Kotlensky, W. V., Fischbach, D. B., and Martens, H. E., "Basal Plane Shear Behavior of Pyrolytic Graphite at High Temperatures," Paper No. V-1 (extended abstract). *Symposium on Carbon,* Tokyo, July 1964.

43. Fischbach, D. B., and Kotlensky, W. V., "Carbon and Graphite Research: Shear Deformation of Pyrolytic Carbons Parallel to the Substrate," in *Supporting Research and Advanced Development,* Space Programs Summary 37-37, Vol. IV, pp. 81 and 82. Jet Propulsion Laboratory, Pasadena, Calif., Feb. 28, 1966.

44. Kotlensky, W. V., "Basal Plane Shear in Pyrolytic Carbon," in *Supporting Research and Advanced Development,* Space Programs Summary 37-35, Vol. IV, pp. 62–64. Jet Propulsion Laboratory, Pasadena, Calif., Oct. 31, 1965.

45. Gifkins, R. C., and Snowden, K. V., "Mechanisms for 'Viscous' Grain Boundary Sliding," *Nature,* Vol. 212, No. 5069, pp. 916 and 917, Dec. 24, 1966.

46. Gifkins, R. C., "Diffusional Creep Mechanisms," *J. Am. Ceram. Soc.,* Vol. 51, No. 2, pp. 69–72, Feb. 21, 1968.